Laboratory 25

X-Ray Microanalysis in the AEM

25.1 Sources of Spurious X-Rays

Radiation emanating from regions of the specimen other than the beam-specimen interaction volume can limit the usefulness of x-ray microanalysis. Two major sources exist: the illumination system and postspecimen scatter. It is possible to observe the presence of these effects and determine if they will limit any proposed experiment.

Experiment 25.1: The "Hole Count." By placing the electron probe down a hole in the specimen (open grid square), spurious sources of radiation (both electrons and x-rays from the illumination system) can be detected because they will generate characteristic x-rays from regions of the specimen far from the beam location. Thus, superimposed upon the true spectrum from under the beam will be a small spectrum associated with the average composition of the entire specimen.

Traditionally, a disk specimen of silver or molybdenum has been used to detect the relative level of the "hole count." However, with a disk specimen the value of hole count measured varied with disk rim thickness and the thickness of foil used for the on-foil spectrum. To avoid this variation we need a thin film of constant thickness supported by a thick grid or aperture. Possible test samples are a chromium film on a gold grid (which we will use) or a chromium film on a molybdenum aperture. We will define the hole count as the ratio of the AuL_α intensity (in the hole) to the CrK_α intensity (on the uniform film). Of course, the values of hole count obtained with different specimens cannot be compared directly. Figure A25A.1 shows an electron-generated chromium on gold spectrum and Figure A25.2 shows a spectrum generated down the hole, primarily by high energy x-rays or bremsstrahlung. Note that the CrK_α/K_β lines disappear but the Au*L* and *M* lines remain.

Using a thick C_2 aperture (0.5 mm platinum) cuts down the stray x-rays to reasonable levels at 100 kV, i.e., below the background intensity in the specimen spectrum. Compare the intensity scale in Figure A25.3 (thick aperture) with Figure A25.2 (conventional aperture). This remedy may not be sufficient at voltages above 100 kV and for specimens of high atomic number.

Experiment 25.2: Postspecimen Scatter. Even if the illumination system is "cleaned up" by using a thick C_2 aperture, x-rays can still be excited from regions of the sample remote from the beam-specimen interaction volume. This is illustrated by the presence of a strong Au*L* peak in the spectrum from the chromium thin film sample. See Figure A25.4 which shows a similar experiment with a thin film of gold on carbon supported on a copper grid. This copper peak was generated at the copper grid, which is many microns from the probe position. The peak arises because of electron scatter within the sample and from the objective aperture or other bulk material below the plane of the sample. Another possible source is specimen-generated bremsstrahlung, but this contribution is thought to be minor.

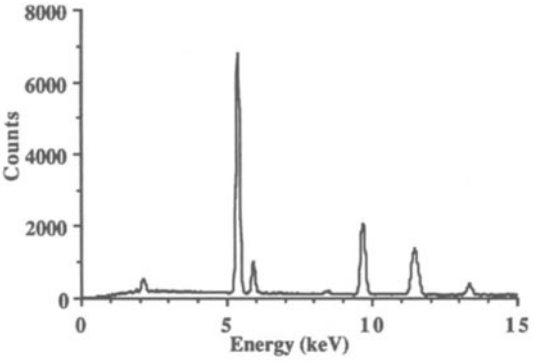

Figure A25.1. Electron-excited spectrum from chromium film on a gold grid showing the CrK_α/K_β lines at ~5.5 keV, the AuL line family at 10-15 keV, and the AuM_α line at ~2 keV.

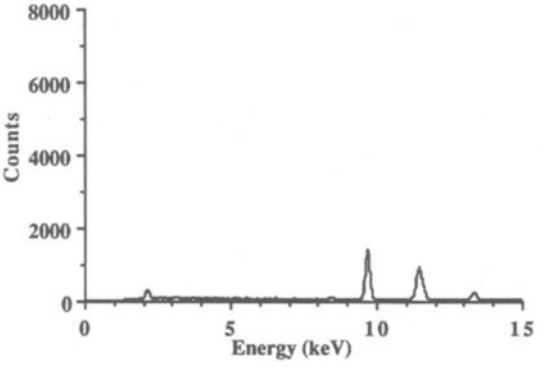

Figure A25.2. The spectrum from the chromium on gold sample, but with the beam down a hole in the sample. The spectrum is generated by high-energy bremsstrahlung from the illumination system which only fluoresces the gold grid.

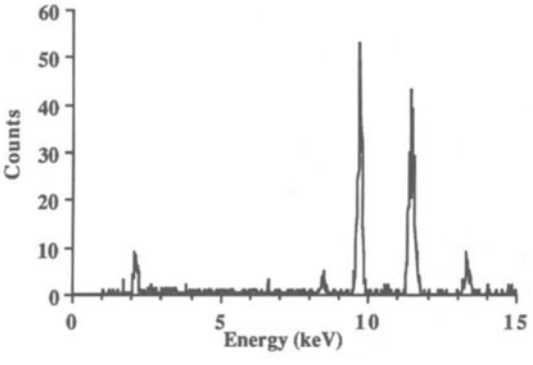

Figure A25.3. Same conditions as Figure A25.2 except a thick PtC_2 aperture was inserted to reduce the flux of bremsstrahlung from the illumination system. The AuL_α intensity is reduced from ~1500 to ~50 counts.

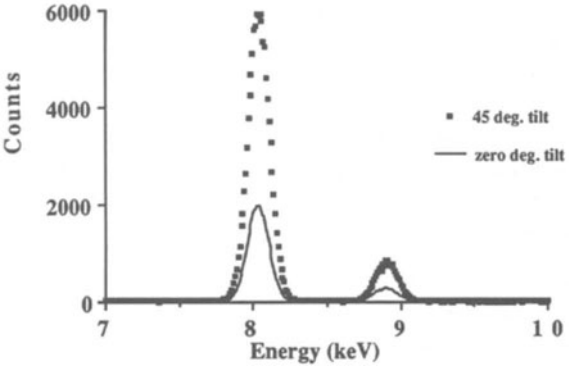

Figure A25.4. CuK_α/K_β lines generated from the support grid when the beam strikes a thin film, several micrometers from the grid bar. The copper lines increase in intensity with higher sample tilts, indicating that increased scattering from the sample is responsible for the CuK_α and K_β peaks.

Tilting the sample increases the gold (copper in Figure A25.4) peak intensity by increasing the amount of gold (copper) grid that interacts with electrons and x-rays scattered by the sample. Other elements in the specimen holder and stage region can also contribute x-rays to the spectrum. These x-rays cannot be distinguished from the x-rays generated by small amounts of the same element present in the sample. Therefore, there is a specific limitation to the analysis of a minor element in any sample for which the element is present as a major constituent in areas of the specimen (or specimen holder) away from the analysis point.

25.2 X-Ray Data Collection

Experiment 25.3: EDS Detector Position with Respect to the Image. It is important to know the direction of the EDS detector axis relative to the sample in order to maintain the smallest x-ray path length (see Figure 25A-5). Pushing on the side-entry goniometer specimen holder uniquely establishes the orientation of the sample to the EDS detector. Once the orientation is determined, always position the sample with the thinnest region towards the detector. Also, if the region around an interface is being analyzed, the interface should be parallel to the EDS axis, especially if x-ray absorption is likely to be a problem. Otherwise, differential absorption of x-rays will occur on one side of the interface.

Experiment 25.4: Collection of X-Rays. When collecting x-rays for quantification, the maximum number of x-ray counts should be obtained in the minimum time. At the same time the detector must not be overloaded. Dead time should be kept below 25%-30%. If the dead time is too large, artifacts such as sum peaks appear in the spectrum and peak shapes become distorted. It is convenient to monitor the count rate in a major peak (e.g., FeK_α) and the dead time, as a function of several variables:

(a) Maximum kV means maximum gun brightness and therefore maximum x-ray generation.

(b,c) Probe current i_p and probe size d_p for a thermionic source are related theoretically by $i_p \sim d_p^{8/3}$ if lens aberrations are the limiting factor. Generally, $i_p = \text{const}\beta\, d_p^2\, \alpha_p^2$ where β is the gun brightness, and so increasing d_p substantially increases i_p, thus increasing the x-ray count rate. In an FEG system the probe size may be changed by the virtual objective aperture (VOA) or by the C_1 lens, but only the VOA changes the current.

(d,e) A larger C_2 aperture increases the probe current with the possibility of an increase in probe size due to spherical aberration. A smaller C_2 aperture results in a well-defined probe, but with a much lower current.

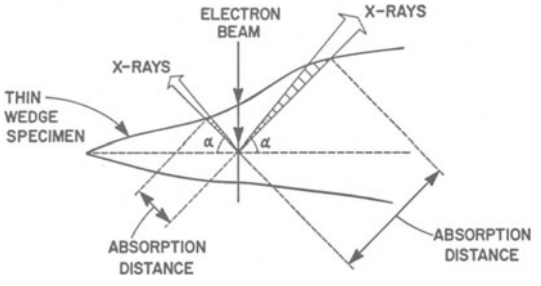

Figure A25.5. The variation in x-ray absorption path length in a nonuniform wedge specimen. If the EDS detector position with respect to the sample is known, then the sample can be oriented so that x-rays follow the shortest path length through the sample prior to detection. Here the EDS detector should be located on the left.

Table A25.1. Results of Quantification Using Different Spectral Manipulation Schemes

	wt% Fe	wt% Ni
Window method (1.2 FWHM) for peaks and averaged background	65.9 ± 1.1	34.1 ± 1.1
Gaussian peak fitting with Kramers' Law background fitting	66.1 ± 1.1	33.9 ± 1.0
Peak fitting using library standards, with digital filtering of background	63.9 ± 1.1	36.1 ± 1.0

Errors are ±3σ (99% confidence limits using counting statistics only).
Specimen is Fe-35% Ni (using electron microprobe bulk analysis).

Experiment 25.5: Background Subtraction. Several techniques may be used for subtracting the background (bremsstrahlung) x-ray intensity from beneath the characteristic peak; for example, computer curve fitting or mathematical filtering methods. However, for a relatively simple spectrum such as that from Fe-Ni neither technique has any advantage over the more primitive methods such as drawing a straight line under the peak (Figure A25.6) or using "windows" on either side of the characteristic peak (Figure A25.7). A comparison of quantification using different background subtraction routines is given in Table 25.1.

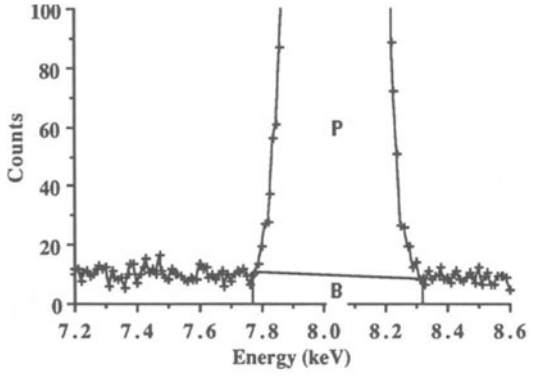

Figure A25.6. Background subtraction under an isolated K_α peak ("gross/net" approach).

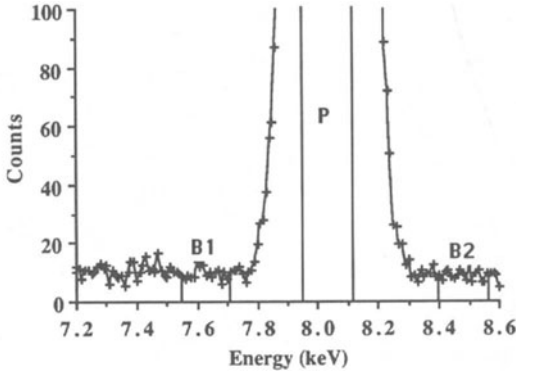

Figure 25.7. Background estimation under an isolated K_α peak by averaging the background intensities in "windows" B1, and B2 on either side of the peak.

25.3 Quantification of Data

Experiment 25.6: Measurement of the k-Factor. Thin foil microanalysis can be very straightforward and often requires only the determination of a k_{AB} factor, using an appropriate standard. Determination of the k_{AB} factor is quite simple if the specimen is sufficiently thin:

1. Use a standard with known amounts of elements in weight percent or atomic percent.
2. Use the same kV for standard and unknown.
3. Use the same detector for standard and unknown.
4. Collect intensity data in identical manner for standard and unknown. Then:

$$\frac{C_A}{C_B} = k_{AB}\frac{I_A}{I_B}$$

5. From the standard obtain the k_{AB} value: $k_{AB} = (C_A/C_B)_{\text{standard}} \times (I_B/I_A)_{\text{standard}}$. Thus, C_A/C_B may be determined for the unknown from $(I_A/I_B)_{\text{unknown}}$ and k_{AB}. The individual elemental fractions C_A and C_B for a two-element system may be calculated from $C_A + C_B = 1$. If no standard is available k_{AB} can be calculated (see *PAEM*, p. 160).

Experiment 25.7: Errors in k-Factor Determination. As in most analysis procedures the error is minimized if the statistics are good. Therefore, the more x-ray counts the better. Thus if there are $N = 10^4$ counts in I_A and I_B, then the standard deviation is

$$\sigma = \sqrt{N} = \sqrt{10^4} = 10^2$$

for both I_A and I_B. Assuming that one wants errors at the "$\pm 3\sigma$" or 99% confidence limit, then 3σ (or more appropriately s_n) $= 3 \times 10^2$. Therefore, the relative error in I_A and $I_B = \pm 3s_n/N = \pm 300/10{,}000 = \pm 3\%$ relative. The total error in k_{AB} is the sum of the errors in I_A and I_B ($\pm 6\%$) plus the error in the standard. Thus, for a k_{AB} measured on a standard that is well characterized (better than $\pm 1\%$ relative accuracy), the total error in k_{AB} may be about $\pm 7\%$. If we collect 10^5 counts from the standard in I_A and I_B, a similar argument leads to an error in k_{AB} of $\pm 3\%$, which is a typical minimum error.

If either component A or B is present in small amounts, then the error in k_{AB} increases rapidly. For example, if there are 10^4 counts in I_A but only 10^3 counts in I_B, then using the same argument as above, $\pm 3s_n$ is $\pm 10\%$ in I_B, 3% in I_A, and the total error in k_{AB} is about $\pm 14\%$ relative.

It should be pointed out that the errors calculated above are overestimates. Since the measurements are statistical in nature, the standard deviations may be summed in quadrature which reduces the level of the relative error by about a third. Thus, the total relative error in a single AEM measurement, where I_A and I_B each contain more than 10,000 counts, is approximately 2/3($\pm 3\%$ in k_{AB} plus $\pm 6\%$ from I_A/I_B) = $\pm 6\%$. Thus, many AEM references in the literature refer to a relative error of about 5%-10% for this technique.

If several independent measurements of the k-factor are made a lower relative error may be calculated using the standard deviation and the "Student's t" distribution. Values for t may be found for several confidence levels in published statistical tables.

Experiment 25.8: Multielement Quantification. Since most materials of interest are not simple binary alloys the quantification can be more tedious. In the sample of biotite, several of the characteristic peaks are very close together in the low-energy region of the spectrum where the background x-ray intensity is changing rapidly (Figure A25.8a). Background subtraction in this case must be done by computer (Figure A25.8b) with appropriate standards and k-factors fed into the computer. Time does not permit all these data

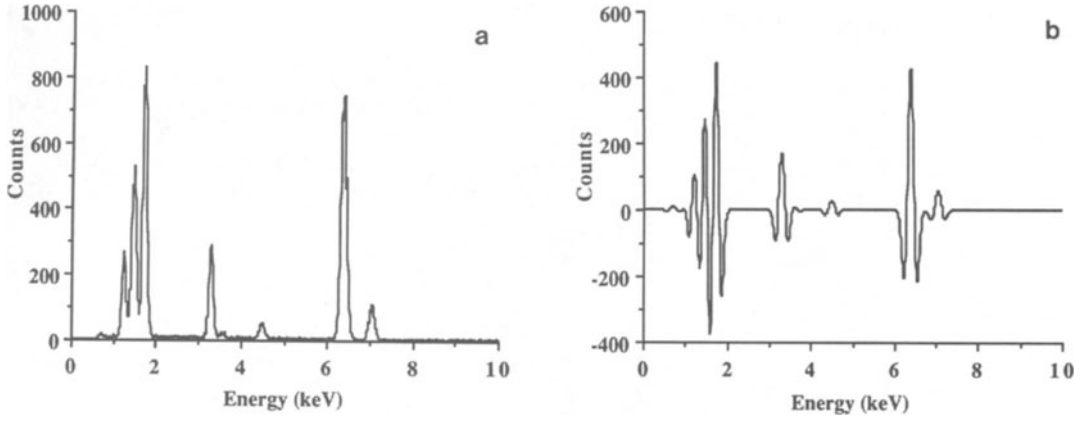

Figure A25.8. (a) EDS spectrum of biotite showing closely spaced peaks. To subtract the background, a mathematical method such as digital filtering is required as shown in (b), which is the result of convoluting spectrum (a) with a "top-hat"-shaped filter function. The background intensity is reduced to zero between the characteristic peaks.

to be gathered during the laboratory session. Quantification using calculated k_{AB} factors can be carried out to give an approximate answer. Compare with the nominal concentration values stated in the experiment. For any microanalysis situation, the "correctness" of our measurements can only be assessed by using various standards as unknowns to check the validity of our methods.

Experiment 25.9: Absorption Correction. The simple Cliff-Lorimer equation has to be corrected if characteristic x-rays are absorbed or fluoresced significantly (correction >10%). In the NiAl specimen, AlK_α x-rays are strongly absorbed and this should be observable as an increase in the Ni/Al intensity ratio as the thickness of the specimen increases.

The equation to correct the collected spectrum is

$$\frac{C_A}{C_B} = k_{AB}\,\frac{I_A}{I_B}\ \text{(A.C.F.)}$$

where

$$\text{A.C.F.} = \frac{\left(\frac{\mu}{\rho}\right)^{A}_{\text{spec}}\left[1\text{-exp}\left(\left(\frac{\mu}{\rho}\right)^{B}_{\text{spec}}\rho\, t\,\text{cosec}\,\alpha\right)\right]}{\left(\frac{\mu}{\rho}\right)^{B}_{\text{spec}}\left[1\text{-exp}\left(\left(\frac{\mu}{\rho}\right)^{A}_{\text{spec}}\rho\, t\,\text{cosec}\,\alpha\right)\right]}$$

where ρ is the specimen density, t is the specimen thickness, α is the x-ray take-off angle, and $\mu/\rho\ A_{\text{spec}}$ is the mass absorption coefficient for element A x-rays absorbed in the specimen. This factor may be determined for nickel in NiAl using a weighted average of mass absorption coefficients:

$$\left(\frac{\mu}{\rho}\right)^{\text{Ni}}_{\text{spec}} = \left(\frac{\mu}{\rho}\right)^{\text{Ni}K_\alpha}_{\text{Ni}} C_{\text{Ni}} + \left(\frac{\mu}{\rho}\right)^{\text{Ni}K_\alpha}_{\text{Al}} C_{\text{Al}}$$

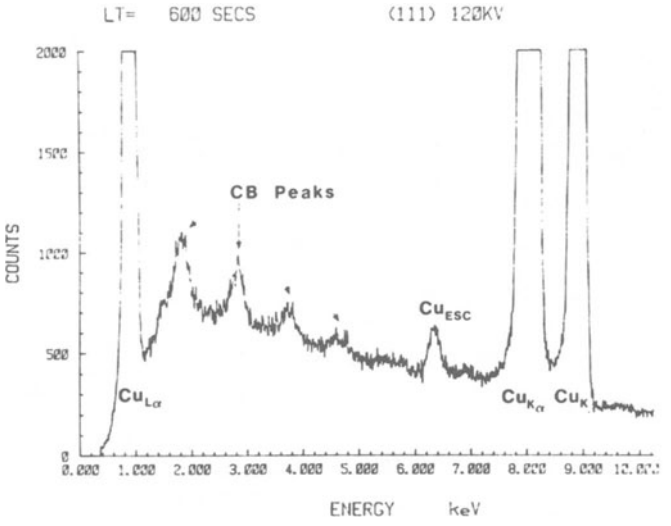

Figure A25.9. A series of copper spectra taken at 120 kV. The CuL, CuK_α, K_β, and copper escape peaks are labeled, but other small Gaussian peaks exist. These peaks are due to coherent bremsstrahlung production.

where C_i is the weight fraction of element i. Stoichiometric NiAl is 68.51 wt% Ni. A similar equation must be developed for aluminum in NiAl. The following values of μ/ρ are required and are taken from Heinrich's Tables [1]:

$$\left.\frac{\mu}{\rho}\right]_{Ni}^{Ni} = 58.9 \text{ cm}^2\text{gm}^{-1}$$

$$\left.\frac{\mu}{\rho}\right]_{Al}^{Ni} = 60.7 \text{ cm}^2\text{gm}^{-1}$$

$$\left.\frac{\mu}{\rho}\right]_{Ni}^{Al} = 4837.5 \text{ cm}^2\text{gm}^{-1}$$

$$\left.\frac{\mu}{\rho}\right]_{Al}^{Al} = 385.7 \text{ cm}^2\text{gm}^{-1}$$

In addition, the specimen thickness t has to be determined, and the take-off angle α and specimen density ρ have to be known. The contamination spot separation method often overestimates the thickness of the specimen and therefore results in overcorrection of the intensity data for absorption effects. In this case, the calculated result will show an excess of aluminum with respect to the known stoichiometric composition of the specimen. If the composition and/or density are unknown, it is necessary to follow an iterative procedure by first estimating C_A and C_B in order to determine an appropriate ρ, and then using this value of ρ in the correction factor equation to calculate a value of C_A and C_B. From these values redetermine ρ and redo the calculation until the result is self-consistent. Most computer programs allow for this iterative procedure.

25.4 Coherent Bremsstrahlung Effects

Experiment 25.10: Detection of Coherent Bremsstrahlung. Coherent bremsstrahlung peaks arise in thin foil specimens under high-voltage irradiation because the sample is usually a single crystal through the analyzed region (see *PAEM*, p. 147). Bremsstrahlung is therefore produced regularly through the periodic crystalline sample and the result is a coherent beam of bremsstrahlung of energy E given by

$$E(\text{kV}) = 12.4\ \beta/L[(1 - \beta \cos (90 + \theta)])$$

where $\beta = v/c$, θ is the take-off angle (assuming the specimen is normal to the beam) and L is the interplanar spacing in the beam direction. Specific gaussian peaks arising from different higher order Laue zone planes are visible at about the 1% intensity level. The peaks move as a function of kV and orientations as predicted by the above equation (see Figure A25.9). These peaks may cause difficulty in measuring grain boundary segregants such as S and P which have peaks of similar intensities at similar energies.

Reference

[1] K. F. J. Heinrich, *The Electron Microprobe*, ed. T. D. McKinley, K. F. J. Heinrich, and D. B. Wittry, Wiley and Sons, New York (1966) 351. Many mass-absorption coefficients from Heinrich's tables are quoted in Goldstein et al., *Scanning Electron Microscopy and X-Ray Microanalysis*, Plenum Press, New York (1981) 624.